

QUASAR: Development of 20 picosecond resolution intensity interferometry

Gilles Koziol,^{a,*} Ivan Cardea,^b Edoardo Charbon,^b Daniel Florin,^d Benjamin Garcia,^a Ludovic Genolet,^a Andrea Guerrieri,^e Etienne Lyard,^a Nicolas Produit,^a Aramis Raiola,^c Prasenjit Saha,^d Vitalii Sliusar,^a Lucijana Stanic,^d Achim Vollhardt,^d Domenico della Volpe^c and Roland Walter^a

^aUniversity of Geneva, Department of Astronomy, Switzerland

^bEcole Polytechnique Fédérale de Lausanne (EPFL), Switzerland

^cUniversity of Geneva, Département de physique nucléaire et corpusculaire, Switzerland

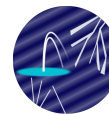
^dUniversity of Zurich, Switzerland

^eUniversity of Applied Sciences Western Switzerland (HES-SO Valais-Wallis)

E-mail: gilles.koziol@unige.ch

In 1956, the pioneering experiment of Hanbury Brown and Twiss (HBT) on measuring the sizes of bright stars was limited by the time resolution of their detectors and their telescope size. Recent developments in single-photon avalanche diodes (SPADs) have lowered detector time resolution to under tens of picoseconds. In this work, we report the results of laboratory tests of SPAD detectors to observe the HBT effect in photon-counting mode. Using a simple laboratory setup and cutting-edge SPAD detectors, we obtain a time resolution of ≈ 20 ps (2 SPADs + TDC). Additionally, using thermal light sources and narrow spectral filters, we analyze the second-order correlation function obtained from different light sources of continuous and line spectra. Results are discussed and compared with the expectations. Furthermore, we report on a setup, allowing to simulate and estimate the size of an artificial star of known size to verify the analysis and data correlation techniques.

39th International Cosmic Ray Conference (ICRC2025)
15–24 July 2025
Geneva, Switzerland



ICRC 2025

The Astroparticle Physics Conference
Geneva July 15-24, 2025

*Speaker

1. Introduction

The pioneer experiment led by Hanbury Brown and Twiss in the 50s opened a new field of astronomy, offering sub-milliarcsecond resolution without having to face atmospheric perturbations [1]. However, it had two major limitations: time resolution (20ns) and the collecting area ($\sim 2m^2$). The recent progress in single photon detection with 6ps resolution [2] motivates a revisit of their experiment. With such enhancement, the same SNR could be obtained with 3000 times less exposure, opening new fields of research in astronomy. The QUASAR project [3, 4] aims at 20ps resolution spectrometer to be placed on the biggest telescopes to reach Event Horizon Telescope-like resolution in visible light.

In this work, we present a compact SPAD-based intensity interferometer. By observing narrow emission lines, we show that the device has a suitable time resolution for our needs and low systematics. Hence, we are able to resolve the 640nm emission line of a Mercury-Cadmium calibration lamp. Additionally, using a pinhole as a fake star that we successfully resolve, we demonstrate that these detectors are ready to be brought to telescopes for stellar measurements.

2. Light coherence

In his paper of 1963 [5], R. Glauber provided a complete and detailed explanation of the result obtained in 1956 by HBT. He later received the Nobel Prize for his work on optical coherence. The whole idea of Glauber is to express the probability of detecting photons at a given time and space interval, using the quantum description of the electromagnetic field. He expresses the coincident photon detection probability (the second-order correlation function) using this formalism. Applied to thermal states, the normalized second-order correlation function can be simplified to the Siegert relation [6]:

$$g^2(\tau) = 1 + |g^{(1)}(\tau)|^2 \quad (1)$$

where $g^{(1)}(\tau)$ is the first-order correlation function, which verifies $g^{(1)}(0) = 1$. The shape of the second-order coherence function is given by the Fourier transform of the lineshape [7]. Additionally, the above coherence is modulated by the square visibility $|V_{12}|^2$, given by the source brightness distribution. For zero baseline condition ($V_{12} = 1$), we have $g^2(\tau = 0) = 2$.

The use of detectors having non-zero jitter implies that the time resolution will convolve the observed coherence. Similarly, the observed visibility is convolved by the aperture of the pupil [8]. An important quantity for all the coherence measurements is the coherence time at zero baseline, which can be computed as follows [7]:

$$\tau_c = \int_{-\infty}^{\infty} d\tau |g^{(1)}(\tau)|^2 \quad (2)$$

Given the lineshape, this information allows us to derive the linewidth of the observed source.

3. Experimental setup

The experimental setup is shown in Figure 1. The light is captured using a lens coupled to a single-mode (SM) optical fibre. After passing the entrance polarizer, the light is split into two,

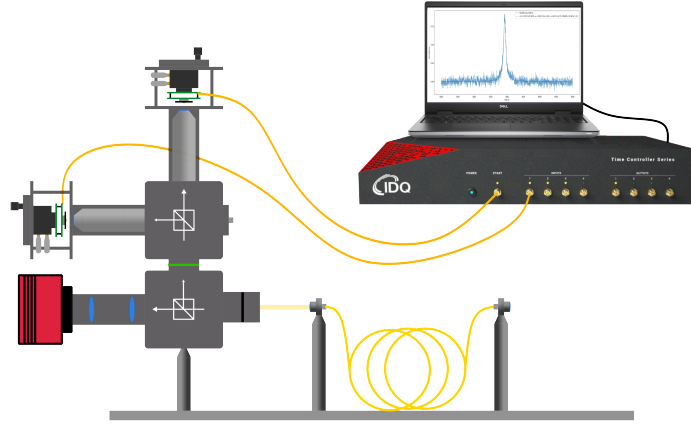


Figure 1: Scheme of the interferometer in the *zero baseline* configuration. The light is injected using a single-mode optical fibre. The light is divided into two branches and the CCD (for visual purposes) using a series of beam splitters. The SPADs are placed after a set of lenses, allowing to focus most of the light on their $25\mu\text{m}$ sensitive diameter. The analog output is directly connected to the input of the ID1000, which provides the photon coincidence with a resolution of 1ps.

between the CCD (for visual purposes) and the two arms of the detector, placed after the filter. The light is equally split between the two branches of the setup using a second beam splitter. The $25\mu\text{m}$ detectors are placed on micrometric XYZ, after a set of lenses, to accurately focus most of the light on the detector to maximize the observed rate. The detectors are SPADs from EPFL [2], which have a single photon detection jitter of 12.1ps FWHM. The analog output is directly connected to the input of the ID1000 *, which provides a digital resolution of 1ps and a measured Gaussian jitter with $\sigma \approx 3.6\text{ps}$. It computes the photon inter-arrival times internally.

We use different kinds of light sources: The LED (OSRAM LE CG P1AQ), for calibration and time resolution measurement, and a Mercury-Cadmium lamp (OSRAM - HgCd/10), having an emission line at 643.85nm. Finally, we also use a Sodium lamp (Philips SOX35W), emitting the well-known Na doublet (589.00/589.59 nm). By tilting a 1nm transmission filter at the entrance of the device, we can select the desired emission line. By adding a linear X translation stage to either one of the two branches, we create an artificial baseline.

4. Experiments

4.1 Timing resolution

A correlated noise is observed, but it can be removed by taking long calibration runs. Once removed, we obtain clean corrected data, such as the blue data points on figure 2, showing the result of $\sim 160\text{h}$ of LED light, filtered by a 1nm filter. The average number of random coincidences is $4.16 \cdot 10^6$ counts per 4ps bin. We build the normalized coincidence counts by dividing the number of counts per bin by the average number of counts per bin outside the peak region.

As the non-zero jitter of the detectors impacts the spread of the observed coherence function, we start by measuring the timing response of the system using the coherence of the LED's green

*<https://www.idquantique.com/quantum-detection-systems/products/id1000-time-controller/>

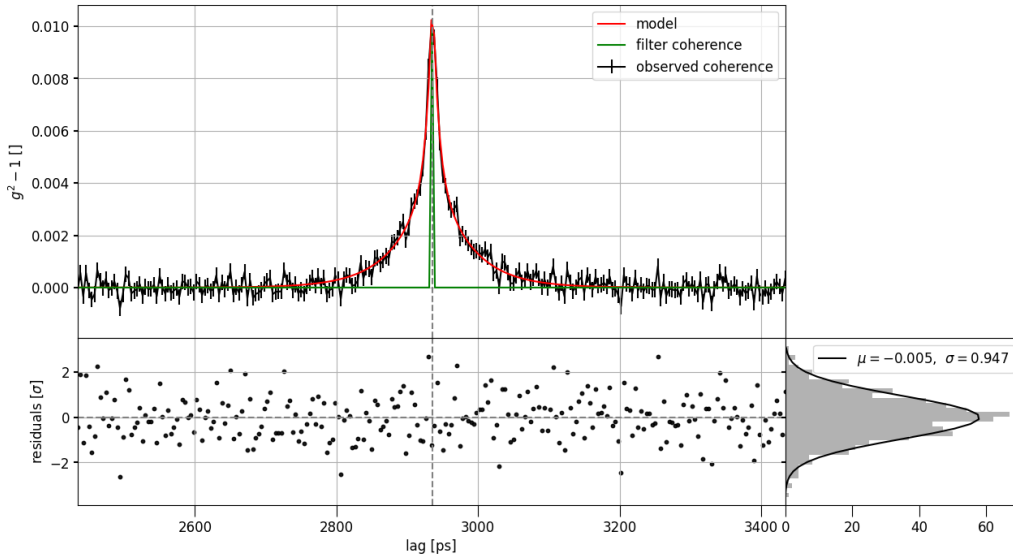


Figure 2: (*black*): Measurement of the measured coincidence normalized count, obtained using the LED light filtered by a 1nm interference filter. (*red*): Jitter model by a sum of two decaying exponentials of the form $e^{-|x|/\tau}$. (*green*): Filter coherence, scaled for visual purposes.

light, filtered by a 1nm filter. The expected coherence time is 0.57ps^\dagger (see the black curve of figure 2), smaller than the TDC's digital resolution. Hence, the observed coherence can be fitted with any suitable model and will be assumed to be the jitter.

We fit the result using a sum of two exponential functions of the form $e^{-|x|/\tau}$. The best fit amplitudes are $4.97 \cdot 10^{-3}$ and $6.74 \cdot 10^{-3}$ and the best fit τ parameters are 47.6 and 7.7ps, respectively. As can be seen in figure 2, this fit provides a good description of the data. It is essential to have a good knowledge of the jitter function (which characterizes the detectors + TDC system), as line deconvolution is an inverse problem and therefore highly sensitive to timing resolution. By integrating the black curve of figure 2, we derive a coherence time of $0.58 \pm 0.02\text{ps}$, in good agreement with the expected value of 0.57ps obtained by integrating the Fourier transform of the filter transmission.

The FWHM was estimated to $\sim 25\text{ps}$, suggesting that we can reach the same SNR as Hanbury Brown and Twiss with roughly 3000 times less exposure.

4.2 640nm Cd line analysis

Using the zero baseline configuration, we analyse the 640.85nm emission line that we assume to have a Lorentzian lineshape. We use the time resolution model as a convolution kernel to infer the amplitude of the intrinsic $g^1(\tau)$ and the emission line width parameter. If the intrinsic amplitude reaches 1, it will demonstrate that all the parameters are under control. Therefore, we built a model assuming a Lorentzian emission line, convolved by the time resolution. The free parameters are the amplitude, the linewidth, and the time offset.

[†]Computed from the available filter transmission data

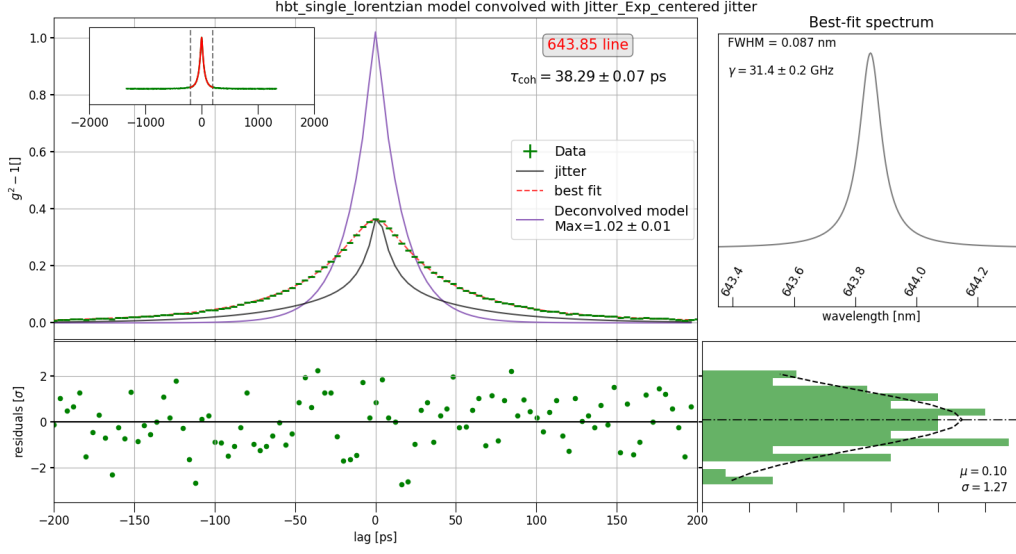


Figure 3: Analysis result of the 643nm Cadmium emission line. The inferred intrinsic $g^{(1)}(0)$ amplitude is estimated to 1.02 ± 0.01 , in good agreement with the single mode expectations. The derived linewidth is 0.087nm, and is shown on the top right panel.

We show in Figure 3 the analysis result for the 643.85nm Cadmium emission line, observed at ~ 2.5 MHz for 4.2 hours. The main result is the deconvolved amplitude 1.02 ± 0.01 , which is in excellent agreement with the expectations. The Lorentzian parameter γ is estimated to 31.5 ± 0.2 GHz, corresponding to a linewidth of 0.087nm FWHM. We also measure the coherence time using equation 2 and derive a value of 38.3 ± 0.1 ps.

4.3 Fake star

Finally, we use a $50 \pm 3\mu\text{m}$ pinhole at a distance of 120cm, illuminated with the Sodium lamp (mimicking a fake star) and a modified version of the setup shown in figure 1 to create a baseline between the two arms of the setup. We assume the pinhole source brightness distribution to be a uniform disk, implying a visibility of the form:

$$V(d) = 2 \cdot \frac{J_1(\pi d \theta_{\text{UD}}/\lambda)}{\pi d \theta_{\text{UD}}/\lambda}, \quad (3)$$

with J_1 the Bessel function of the first kind, θ_{UD} the angular diameter of the source, $d = \sqrt{u^2 + v^2}$ the baseline and λ the observed wavelength. The model predicts, given an angular diameter, the observed squared visibility for each baseline by convolving the obtained $|V(u, v)|^2$ map with the circular aperture of each branch, which has a diameter of 6mm.

We varied the baselines by 18mm. For each baseline, we record the coincidences from the illuminated pinhole and compute the coherence time. The results for each baseline and the fit are shown in Figure 4. The inferred pinhole diameter is $48.1 \pm 2.8\mu\text{m}$, in good agreement with the manufacturer's value. The best fit parameters indicate an offset of 0.05cm between the two branches of the setup.

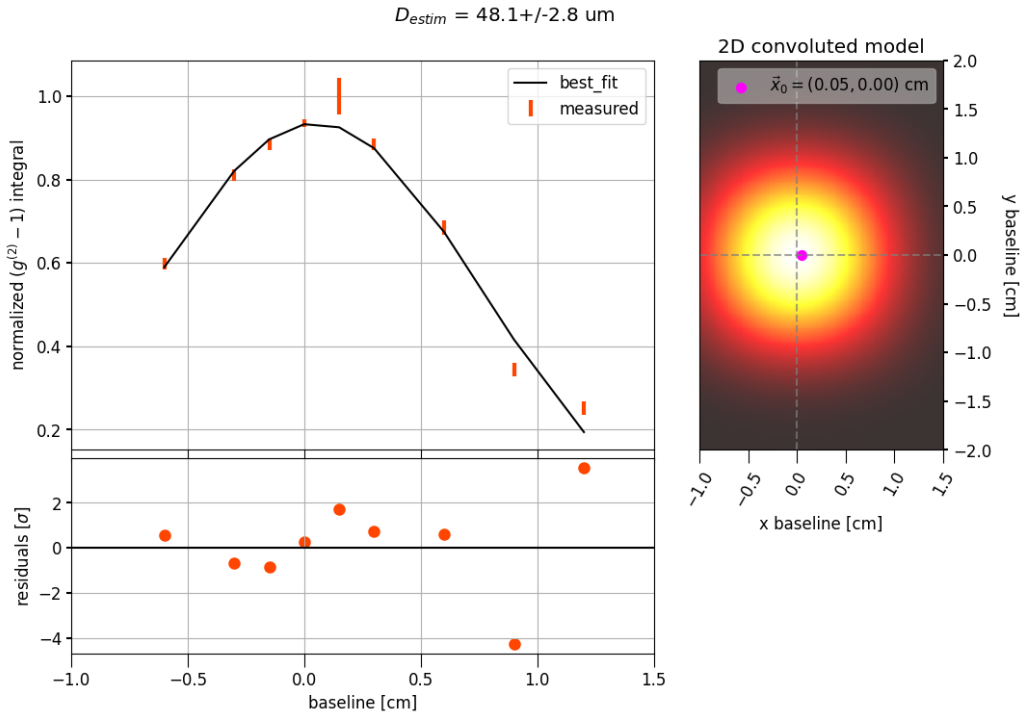


Figure 4: Normalized $(g^{(2)}-1)$ integral as a function of the baseline. Taking into account the 6mm circular pupils and the distance of 120cm, we derive a pinhole diameter of $48.1 \pm 2.8\mu\text{m}$. Points having a large uncertainty were integrated for less than 30 minutes.

The resolved fake star has an angular diameter of roughly 8.6 arcsecond. This value is larger than the angular diameter of stars, but we used small baselines compared to these between two telescopes.

5. Conclusion

First, we have successfully measured the system time resolution of the SPADs+TDC of $\sim 25\text{ps}$ FWHM. Then, using the 643nm Cadmium narrow emission line, we measured a maximum $g^{(2)}(0)$ amplitude of 1.36 and an intrinsic amplitude of 2.02 ± 0.01 , in excellent agreement with the expectations. The pull value of σ is close to one, and demonstrates that we have no significant systematics, allowing us to resolve this line with good accuracy. Finally, we varied the baseline between the two arms of the setup to measure the change in the $g^{(2)}$ integral. We derived a pinhole diameter of $48.1 \pm 2.8\mu\text{m}$, in agreement with the manufacturer's data ($50 \pm 3\mu\text{m}$).

The perfect match between observations and expectations and the negligible systematics are very promising for the use of these detectors for intensity interferometry on telescopes.

References

- [1] Hanbury Brown, R. and Twiss, R. Q. , A Test of a New Type of Stellar Interferometer on Sirius , Nature 178 p.1046-1048 (1956) , [10.1038/1781046a0](https://doi.org/10.1038/1781046a0)
- [2] Gramuglia, Francesco and Wu, Ming-Lo and Bruschini, Claudio and Lee, Myung-Jae and Charbon, Edoardo , A Low-Noise CMOS SPAD Pixel With 12.1 Ps SPTR and 3 Ns Dead Time , IEEE Journal of Selected Topics in Quantum Electronics 28 p.1-9 (2022) , [10.1109/JSTQE.2021.3088216](https://doi.org/10.1109/JSTQE.2021.3088216)
- [3] R.Walter et al. , Reaching 10 microarcsecond in the optical to resolve accretion disks , Proceedings of Science, ICRC 2025 <https://pos.sissa.it/501/975/pdf>,
- [4] R.Walter et al. , Resolving accretion disks with quantum optics , Proceedings of Science, ICRC 2023 <https://doi.org/10.22323/1.444.1491>,
- [5] Glauber, Roy J. , The Quantum Theory of Optical Coherence , Phys Rev 130 p.2529-2539 (1963) , [10.1103/PhysRev.130.2529](https://doi.org/10.1103/PhysRev.130.2529)
- [6] Dilleys Ferreira et al. , Connecting field and intensity correlations: The Siegert relation and how to test it , Am. J. Phys. 88, 831–837 (2020) , <https://doi.org/10.1119/10.0001630>
- [7] Loudon, Rodney , The Quantum Theory of Light , Oxford University Press (2000) doi.org/10.1093/oso/9780198501770.002.0001,
- [8] A. Richard Thompson , James M. Moran , George W. Swenson Jr. , Interferometry and Synthesis in Radio Astronomy , Springer Cham (2017) , doi.org/10.1007/978-3-319-44431-4
- [9] Brown, R. Hanbury and Davis, J. and Allen, L. R. , The Stellar Interferometer at Narrabri Observatory—I: A Description of The Instrument and the Observational Procedure , MNRAS 137 p.375-392 (1967) , [10.1093/mnras/137.4.375](https://doi.org/10.1093/mnras/137.4.375)